Chaotic dynamics in shear-band-mediated plasticity of metallic glasses

Baoan Sun,[1,2,*] Liping Yu,[3,*] Gang Wang,[4] Xing Tong,[4] Chuan Geng,[4] Jingtao Wang,[5] Jingli Ren,[6,†] and Weihua Wang[1,2,‡]

[1]*Institute of Physics, Chinese Academy of Sciences, Beijing 100190, China*
[2]*Songshan Lake Materials Laboratory, Dongguan, Guangdong 523808, China*
[3]*College of Science, Henan University of Technology, Zhengzhou 450001, China*
[4]*Laboratory for Microstructures, Institute of Materials, Shanghai University, Shanghai 200444, China*
[5]*Herbert Gleiter Institute For Nanoscience, Nanjing University of Science and Technology, Nanjing 210094, China*
[6]*Henan Academy of Big Data, Zhengzhou University, Zhengzhou 450052, China*

(Received 13 February 2020; revised manuscript received 26 May 2020; accepted 2 June 2020; published 16 June 2020)

The chaotic dynamics describes how a small change of initial conditions can result in a large difference in a deterministic nonlinear system, i.e., the "butterfly effect." Through a combination of experimental and theoretical analysis, here we showed unambiguously that the deformation of metallic glasses (MGs) exhibits such an effect where the experimentally observed plasticity displays a large plasticity fluctuation under the normally same conditions. The "butterfly effect" for the plasticity of MGs is related to the chaotic dynamics of a shear band, evidenced by the existence of a torus destroyed phase diagram, a positive Lyapunov exponent, and a fractional Lyapunov dimension. Physically, the chaotic shear-band dynamics arises from the interplay between structural disordering and temperature rise within the shear band, which could lead to an uncertainty in the appearance of the critical condition for runaway shear banding events. Our results provide a perspective on the plasticity of MGs from the viewpoint of complex dynamics and are also important for evaluating the plastic deformation properties of MGs in practical applications.

DOI: 10.1103/PhysRevB.101.224111

I. INTRODUCTION

Arising from the long-range disordered atomic structure, the plastic flow of metallic glasses (MGs) or other disordered solids is completely different from that of crystalline materials [1,2]. At atomic scale, the plastic flow of MGs is found to initiate from some loosely packed atomic-scale regions or soft spots [3–5], which are often correlated by long-range elastic interactions and thus can be organized into cascade or avalanchelike events [6,7]. After plastic yielding, these local regions could further concentrate plastic strain, ultimately resulting in strong flow localization, i.e., the plastic strain is highly localized into shear bands [8,9]. The shear banding process could have a profound effect on their macroscopic mechanical behavior. One direct consequence is that a shear band tends to become runaway with the work softening during deformation [10], resulting in the catastrophic failure of MGs. As a result, the poor ductility/plasticity of MGs has become one of main obstacles impeding their widespread applications [11–13]. Meanwhile, the plastic shear of MGs also resembles many important phenomena in natural science and engineering, such as lubrication [14], friction [15], and earthquakes [16]. Despite the fundamental and engineering importance, a comprehensive understanding on the plastic flow process and its correlation with the macroscopic plasticity in MGs are still lacking.

The dynamics of shear banding process has an important effect on the macroscopic plasticity of MGs. Under tension, a shear band will quickly propagate and become unstable under a tensile stress, leading to almost zero plastic deformability of MGs. However, some MGs could display some plasticity, where a shear band often proceeds in a stable and intermittent manner [17–19]. It was found that there is a close correlation between shear-band stability and the overall plasticity in MGs. Extensive studies showed that the instability of a shear band is controlled by a critical parameter, such as a critical shear velocity or a critical elastic energy density released during a serrated event [20,21]. The shear-band instability was also shown to depend on various intrinsic material properties and extrinsic experimental factors, e.g., chemical composition [22], sample size [23,24], loading rate, and even testing machine stiffness [25,26], which ultimately affect the plasticity of MGs. The shear band also has a thickness ranging from a few nms to at least 200 nms depending on the plastic strain [27], indicating a strong sensitivity of the shear band instability or the final plastic strain on the mechanical boundary conditions. There is also some evidence showing that the plasticity of MGs is closely related to the shear-band dynamics, i.e., the chaotic dynamics or self-organized critical dynamics [28,29]. To account for these effects, a number of phenological theories or criteria were proposed, such as the Poisson's ratio criterion for the intrinsic plasticity of MGs [22] and the shear-band instability index [10,25].

*These authors contributed equally to this work.
†renjl@zzu.edu.cn
‡whw@iphy.ac.cn

 ©2020 American Physical Society

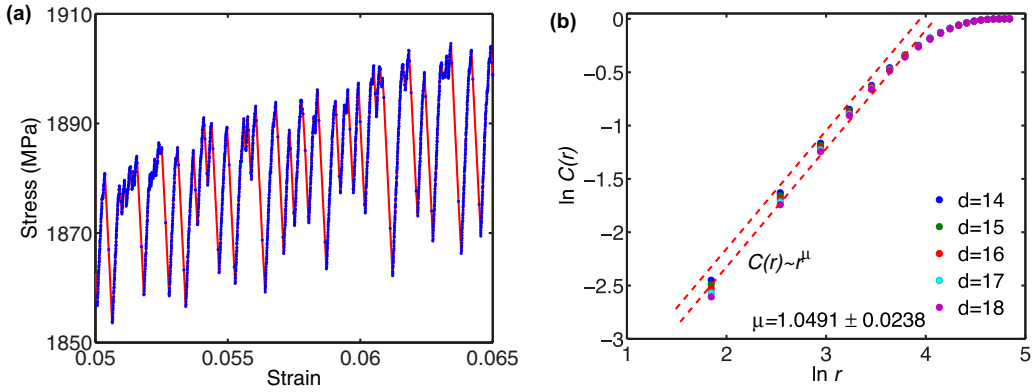

FIG. 2. Time series analysis on the stress-time/strain signals of Vit105 MG. (a) A typical stress-strain segment for time series analysis. (b) The calculated correlation integral $lnC(r)$ versus the distance r, plotting in the log-log form, for the embedding dimension $d = 14$–18. The data points can be well fitted by the equation $C(r) \sim r^{\mu}$ with the fitting exponent $\mu = 1.05$.

of Weibull modulus m often indicates a large variability of the material property and vice versa. Here, the values of m by fitting the plasticity data is about 1.14, which is lower than that reported for other MGs in previous studies [30]. The low value of m found here indicates the significant variability on the shear-band instability for the present MG. We also performed the statistics on the exothermic enthalpy of the sub-T_g relaxation, ΔH_e, and the yield strength σ_y over these specimens (for details see Figs. S4 and S5 in SM [37]). One can see that the distribution of both ΔH_e and σ_y are well fitted by the Weibull function. The value of Weibull modulus m, by fitting the ΔH_e data for the current Vit105 MG is 5.42, which is very close to that of $Zr_{65}Cu_{15}Ni_{10}Al_{10}$ MG ($m \sim 4.1$) reported by Yu *et al.* [30]. The fitting value of m for the σ_y data of Vit105 MG is 24.2, which is smaller than that of $Zr_{65}Cu_{15}Ni_{10}Al_{10}$ MG ($m \sim 41.2$), but is comparable to that of the brittle $(Zr_{48}Cu_{45}Al_7)_{98}Y_2$ MG [43]. Both ΔH_e and σ_y are related to the free volume content in the as-cast samples [44]. The value of m for ΔH_e and σ_y are much larger than that of plasticity, indicating the high uniformity of the initial free volume contents over as-cast MG samples. There seems no structural reason for the observed large plasticity fluctuation.

B. Time series analysis on stress-time curves

In the plastic deformation regime, the MG exhibits obvious serrated flow behavior after yielding, as can be seen in enlarged segments of stress-time/strain curves [Fig. 2(a)]. The serrations are characterized by repeated cycles of sudden stress drops followed by slow upward elastic loading. As extensively studied in literature [17,28,45], serrated flow is closely correlated with the intermittent shear banding process in MGs. Especially for those MGs deformed by a single dominant shear band, serrated flow has been shown to arise from the stick-slip motion of the band along the primary shear plane [26]. To uncover the underlying shear band dynamics, we performed nonlinear time series analysis on serrated stress-time signals. The method is particularly useful to extract the hidden dynamic information of a system from its irregular time noise series. Here, we calculated two parameters: the correlation dimension and the Lyapunov exponent, which are often used to quantify the strange attractor with self-similar properties and the sensitivity to initial conditions of the system [46], respectively. Given a scalar time series measured in units of sampling time $\delta t[x(k), k = 1, 2, 3, ...N]$, one can construct d-dimensional vectors: $Y_k = [x(k), x(k+\tau), ..., x(k+(d-1)\tau)]$, where τ is the delaying time and can be obtained from the autocorrelation time or from mutual information [38]. The correlation integral is calculated as [47] (see Methods for details):

$$C(r) = \frac{1}{N_p} \sum_{i,j} \Theta(r - |Y_i - Y_j|), \tag{1}$$

where Θ is the step function and N_p is the number of vector pairs summed. For a self-similar attractor $C(r) \sim r^{\mu}$ in the limit of small r, where μ is the correlation dimension. The Lyapunov exponents are calculated by the Wolf's method [40]:

$$\lambda_1 = \frac{1}{t_M - t_0} \sum_{k=1}^{M} \ln \frac{L'(t_k)}{L(t_{k-1})}. \tag{2}$$

Here, M is the total number of repeated steps. $L'(t_k)$ and $L(t_{k-1})$ are two distances defined in Methods. For the dynamical system, the spectrum of Lyapunov exponents can be calculated by Benettin algorithm [48], which is equivalent to Wolf's method. Then Lyapunov dimension can be obtained by [41],

$$D_L = j + \frac{\sum_{i=1}^{i=j} \lambda_i}{|\lambda_{j+1}|}, \tag{3}$$

where j is the largest integer such that $\sum_{i=1}^{i=j} \lambda_i \geqslant 0$.

With equations above, we analyzed a typical serrated stress-time curve of Vit105 MG. Figure 2(b) displays the variation of correlation integral, $C(r)$ with the distance r for different embedding dimensions. It can be seen that the slopes of $\ln C(r)$ versus $\ln r$ converge to 1.05 as the embedding dimension reaches $d = 14$. Thus the correlation dimension is taken to be $\mu = 1.05$, indicating the self-similar strange attractor for time-stress signals. In addition, the calculated Lyapunov spectrum also exhibits positive maximum exponents ($\lambda_1 = 0.0321$). The existence of a finite correlation dimension and a

stable positive Lyapunov exponent strongly suggests that the serrated stress signal has chaotic dynamics.

C. Theoretical modeling and analysis

We attempt to understand the above results from the complex dynamics of a single shear band. This is consistent with the experimental facts that the deformation of most MGs are mainly dominated by a single primary shear band during compression [17,45]. The first step is to construct a set of dynamic equations of the shear band, which can fully describe its motion and internal evolution. Previous studies [26,49] have proposed a stick-slip dynamic model to explain the origin of serrated flow in MGs. The model considers that the elastic energy released in the sample-machine system as the driving force for shear-band motion, while the plastic energy is mainly dissipated as configurational entropy or structural disordering within the shear band. The dynamic equations in the model are written as [26]:

$$\frac{d\sigma_b}{dt} = k(v_0 - \lambda_b \dot{\epsilon_b}), \tag{4}$$

$$\frac{d\chi}{dt} = \frac{\dot{\epsilon_b}\sigma_b}{c_0}\left[1 - \frac{\chi \ln(\dot{\epsilon_c}/\dot{\epsilon_b})}{\chi_w}\right], \tag{5}$$

where v_0 is the loading rate, k is the effective elastic constant of sample-machine system, χ is the effective disorder temperature, and σ_b and $\dot{\epsilon_b}$ are the stress resistance and strain rate in the shear band, respectively. χ is the effective disorder temperature [49], which describes the internal state evolution within the shear band. χ could reach a stable state $\chi_w/\ln(\dot{\epsilon_c}/\dot{\epsilon_b})$ for a constant $\dot{\epsilon_b}$. The definition of other parameters can be found in Ref. [24]. The constitutive relation between $\dot{\epsilon_b}$ and σ_b is given by the cooperative shear model (CSM) [50]: $\dot{\epsilon_b} = \dot{\epsilon_s}\exp(-1/\chi)\exp[-W_0(\sigma_{b0} - \sigma_b)^{(3/2)}/(k_B T)]$, where W_0 and σ_{b0} are the critical energy barrier for shear transformation zones (STZs) and the yield strength of the glass at 0 K, respectively. The term $\exp(-1/\chi)$ is proportional to the number density of STZs.

The above model could predict the appearance of serrated flow for shear banding, which is related to a critical stiffness parameter. However, the serrations calculated by this model only have a periodic solution with a fixed size. To fully reveal the complex shear-band dynamic, here we extend the above model by considering the temperature evolution within the shear band. In principle, there should be some temperature gradient within a shear band from its center to boundaries. Here, we assume the shear band as a thin layer with homogeneous temperature distribution. In this case, the flow of heat energy (per unit time and per unit area) across the shear-band boundary is proportional to $K\Delta T/a$, where $\Delta T = T - T_R$ is the instantaneous temperature difference between the shear band (with a temperature T) and glassy matrix (with room temperature T_R), K is thermal conductivity, and a is a characteristic length with the same order of magnitude as shear band thickness. Meanwhile, the heat energy is also produced within the band by the work done by plastic deformation. The dynamic equation for temperature evolution reads:

$$\frac{d\Delta T}{dt} = \frac{\alpha\sigma_b\dot{\epsilon_b}}{\rho c_p} - \frac{K\Delta T}{a}, \tag{6}$$

where ρ and c_p are the density and the heat capacity of the glass material, respectively, and α is the fraction of plastic work dissipated as heat.

Equations (4)–(6) describe the dynamics of a single shear band under compression. Here, χ and ΔT are two internal state variables, k and v_0 are two parameters which can be adjusted, while other parameters are set as constants. We perform a thorough theoretical analysis and numerical calculations on the dynamic model. For analysis details, one can see Text SI in the SM. The results show that the shear band dynamic exhibits a chaotic state within some range of k and v_0. A typical example for $k = 2000$ and $\dot{\epsilon_0} = 10^4$ ($\dot{\epsilon_0}$ is defined by $\dot{\epsilon_0} = v_0/\lambda$) is shown in Fig. 3. As can be seen, the self-similarity of attractor and sensitivity to initial conditions of the chaotic state are characterized by the positive largest Lyapunov exponent ($\lambda_1 = 0.2489$) and Lyapunov dimension ($D_L = 1.2047$). The self-similar torus destroyed phase diagram and the irregular invariant of Poincaré map [Figs. 3(b) and 3(c)] also imply a chaotic state. Arising from the chaotic dynamics, the history diagrams of σ_b with time display serrations with multiple magnitudes of stress drops, as shown in Fig. 3(d). These characteristics are very similar to those of hopping type-B bands in Portevin-Le Chatelier (PLC) effect [51]. It is worth noting that with the chaotic dynamics was also reported by Lemaître in the boundary lubrication by using a full generalization of STZ theory as the constitutive equations [52], which is similar to the stick-slip shear band dynamics observed here.

In addition to the chaotic dynamic state, the shear band dynamics also has a periodic solution when the external strain rate $\dot{\epsilon_0}$ and the elastic constant k are decreased. For the sake of discussion, we replace σ_b with $u = \sqrt{1 - \sigma_b}$ as a new variable, while keep χ and ΔT unchanged. From the theoretical analysis shown in Text SI in SM, (u, χ, ΔT) has a positive equilibrium point E_3. For $\dot{\epsilon_0} = 10^3$ and $k = 100$, E_3 has a value (0.3256, 0.2063, 0.01341) with characteristic roots $\mu_1 = -9.18 \times 10^4$ and $\mu_{2,3} = \pm 0.128i$, indicating Hopf bifurcation emerging at E_3. There are two special points where degenerate Hopf bifurcation occurs: $k = 92.69$, $\dot{\epsilon_0} = 202.35$ and $k = 1000$, $\dot{\epsilon_0} = 0$. Figures 4(a) and 4(b) display the bifurcation diagram of the model with k and $\dot{\epsilon_0}$, respectively. From these diagrams, one can see that the supercritical Hopf bifurcation arises at the point $k = 100$, $\dot{\epsilon_0} = 1415.8$. The Hopf bifurcation is initially subcritical and then becomes supercritical with increasing value of $\dot{\epsilon_0}$, while the direction of Hopf bifurcation cannot change with varying k. In nonlinear dynamics, Hopf bifurcation is often associated with the emergence of limit cycle. Figure 4(c) displays limit cycles initiated from Hopf bifurcation for values of k and $\dot{\epsilon_0}$ in the present model. The existence of limit cycles clearly suggests the periodic oscillation in the system. The periodic solution can also be verified by the numerically calculated time profile of σ_b, which shows periodic stress serrations with a fixed size [Fig. 4(d)].

IV. DISCUSSION

From experimental and theoretical analysis above, one can see that a shear band could exhibit complex nonlinear dynamics including chaos and periodic orbit. These dynamics

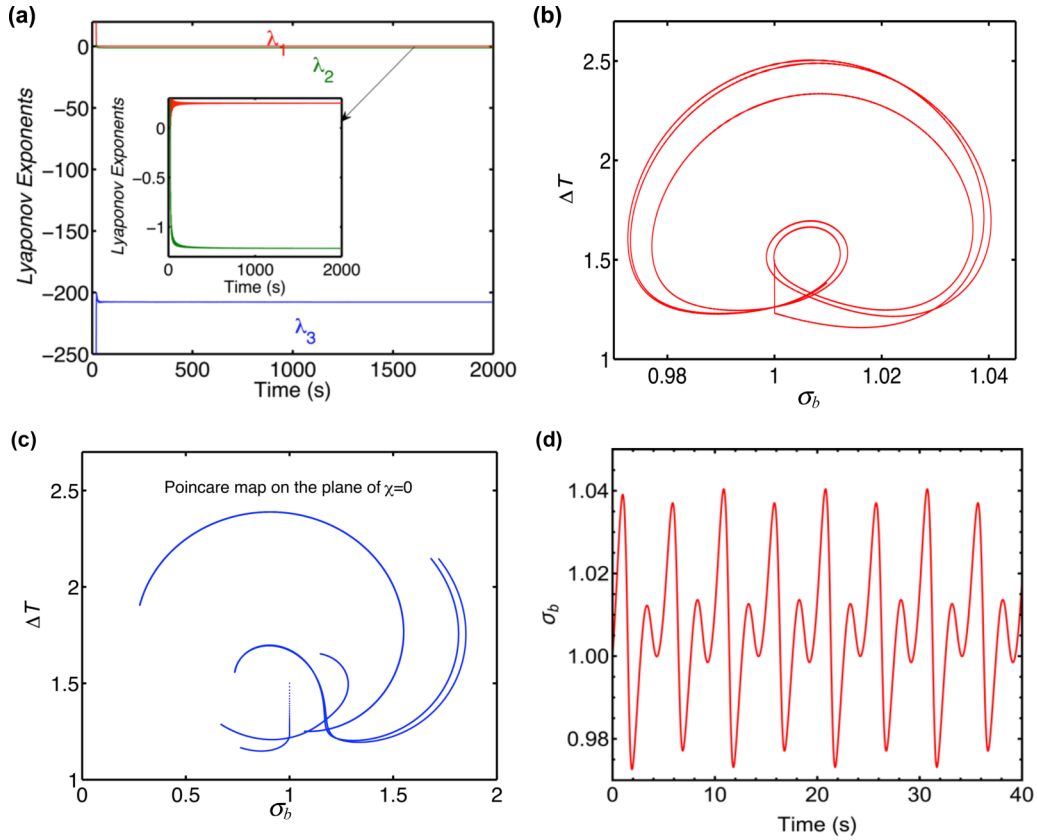

FIG. 3. Chaotic dynamics of a single shear band. (a) Plot of Lyapunov exponent spectrum. The inset is the local amplification for the spectrum. The largest Lyapunov exponent $\lambda_1 = 0.2489$. (b) The phase diagram in the plane of $\sigma_b - \Delta T$, showing a self-similar destroyed torus. (c) Poincaré map on the plane of $\chi = 0$ with an irregular invariant. (d) Time history diagram of σ_b calculated under the initial condition (1, 0.4, 1.5). All results are calculated at the same parameter values: $k = 2000$, $\dot{\epsilon_0} = 10^4$, $\dot{\epsilon_s} = 10^6$, $\dot{\epsilon_c} = 10^5$, and $\beta = 10^4$.

behaviors should have a profound effect on the shear-band stability and the ultimate plasticity of MGs. Now let's discuss the correlation between the chaotic shear-band dynamics and the plasticity fluctuation observed in experiments. Previous studies showed that the stability of a single shear band can be related to a critical parameter, such as a critical shear velocity [21] or a critical elastic energy density [20] released during a serrated event. Once a shear band reaches the state set by the critical parameter, a runaway "defect"(such as cavitation or microcracking) will be developed within the band according to recent studies [53], resulting in the catastrophic materials failure. The plastic strain at which the critical state appears within the shear band defines the macroscopic plasticity of MGs. Since shear banding process in compression often proceeds in a stick-slip manner, so the critical state for shear band can be associated with a critical serrated event. According to our present analysis, if the shear band dynamics is chaotic, the appearance of the critical state for the shear-band instability will be sensitive to initial conditions. Practically, there will be tiny differences (e.g., on chemical compositions, free volume contents, sample size, small deformation due to the bending within a shear band [54,55], etc) due to experimental errors during sample preparation and testing process. These tiny differences will lead to slightly different initial conditions for the shear banding and eventually are enlarged through the inherent chaotic dynamics. As a result, the appearance for the critical state at which the shear band become runaways is unpredictable during deformation, resulting in the large plasticity fluctuation of MGs, as observed in experiments. The chaotic dynamic behavior of shear band found in MGs is reminiscent of the "butterfly effect" as observed in many complex dynamic systems [36], e.g., a butterfly flapping its wings in Brazil can cause a hurricane in Texas.

To further illustrate the "butterfly" effect in the shear-band mediated plasticity in MGs, we numerically calculated the evolution of various variables of shear band with time in the chaotic dynamics regime, as shown in Fig. 5. As can be seen, when the initial conditions of $(\sigma_b, \chi, \Delta T)$ are slightly changed from (0.91, 0.1975, 0.013) to (0.91, 0.2, 0.013), the evolution of $\dot{\epsilon_b}$ within the shear band can be significantly changed after $t = 600s$. Particularly, the serrated event with the largest value of $\dot{\epsilon_b}$ which may cause the instability of shear banding occurs at different times. By arbitrary choosing the critical strain rate for the shear-band instability as $\dot{\epsilon_b} = 4500$, we made statistics on the critical time t_c for the occurrence of shear-band runaway event over a large number of parameter sets of initial conditions. The probability distribution of t_c follows the Weibull distribution well [see Figs. 5(c) and 5(d)], in accordance with experimental results. The numerical calculations further confirm the deterministic nature of the complex shear band dynamics. As the elastic constant k and the external strain rate $\dot{\epsilon_0}$ are decreased, the chaotic dynamics of the shear band is gradually transformed to the periodic orbit. The periodic state is not so sensitive to initial conditions

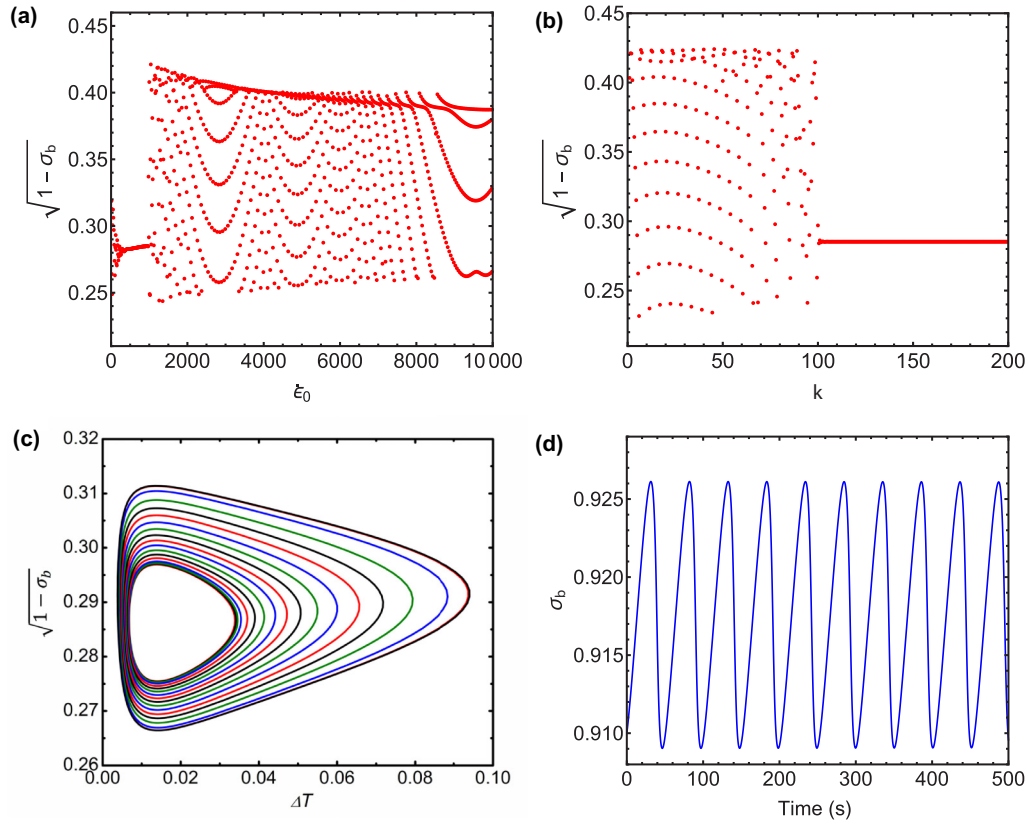

FIG. 4. Periodic dynamics of a single shear band (a) The calculated bifurcation diagram of the model with $\dot{\epsilon}_0$ in the range of $[1, 10^4]$ for $k = 100$, $\dot{\epsilon}_s = 10^6$, $\dot{\epsilon}_c = 10^5$, and $\beta = 10^5$ under initial condition (0.91, 0.2, 0.013). (b) The calculated bifurcation diagram of the model for $\dot{\epsilon}_0 = 10^3$, $\dot{\epsilon}_s = 10^6$, $\dot{\epsilon}_c = 10^5$, and $\beta = 10^5$ under initial condition (0.91, 0.2, 0.013). From these diagrams, one can see that Hopf bifurcation is initially subcritical and then becomes supercritical with increasing value of $\dot{\epsilon}_0$, while the direction of Hopf bifurcation cannot change with varying k. (c) The limit cycles bifurcated by Hopf bifurcation. (d) The time history diagram of σ_b corresponding to the periodic orbit.

and should correspond to the smaller plasticity fluctuation for the same MG. It should be noted that the dynamic states (chaos and periodic orbit) are only limited to the case of a single dominant shear band. In this case, the probability density distribution for the serration size displays a Gauss-like or peak type distribution. For some special ductile MGs, they could form a large number of multiple shear band simultaneously at the initial plastic deformation stage, and the plasticity is often related to a self-organized critical (SOC) dynamics arising from the interaction of a large number of multiple shear bands [28,46]. For the SOC dynamics, the probability density distribution of serration size often follows a power-law scaling, indicating scale-free shear avalanches.

In general, the simple chaos requires at least three variables in a dynamic system [32]. In previous stick-slip models, the effective disorder temperature is considered as the only state governing the internal evolution of the shear band. In these cases, serrations formed by stick-slip shear banding show a periodic behavior [26] rather than a chaotic behavior. In our model, in addition to the effective disorder temperature, we also consider the temperature rise as an internal state variable. The effective disorder temperature is a measure of the STZ density during deformation [56] and in fact is a reflection of the structure disordering in MGs. Thus, the interplay between structural disordering and the temperature rise during deformation must play an important role in the formation of chaotic shear band dynamics. In literature [1,8], the structural disordering as a main cause for strain softening in MGs is well recognized, yet the temperature rise within the shear band has long been debated. By spatially and temporally resolved measurement on shear band velocity, recent studies [57] showed that the maximum temperature rise during shear band propagation is only a few tens of Kelvins. This temperature rise is not enough to cause the significant softening of glassy materials. Therefore, the thermal effect is often believed to be a consequence of strain softening, rather than its main cause before the final fracture of MGs. The effect of temperature rise on the strain softening is also neglected in many theoretical models for shear localization [3–5]. However, our present analysis showed that the role of temperature rise cannot be neglected in shear band dynamics, especially in complicating shear band dynamics. From numerical calculations on our model, we can see that for the periodic orbit state, the calculated temperature rise ΔT is small, in the range of (0.01–0.15) T_R, while for the chaotic dynamic state, ΔT could reach 2.5 T_R, a value sufficient to cause the runaway instability of the shear band. The large temperature rise clearly results from the "butterfly effect" of shear band dynamics. In the chaotic dynamic regime, the small initial temperature rise can be amplified through interplaying with the internal stress and the structural disordering in the shear band. Conversely, the temperature rise also modulates the

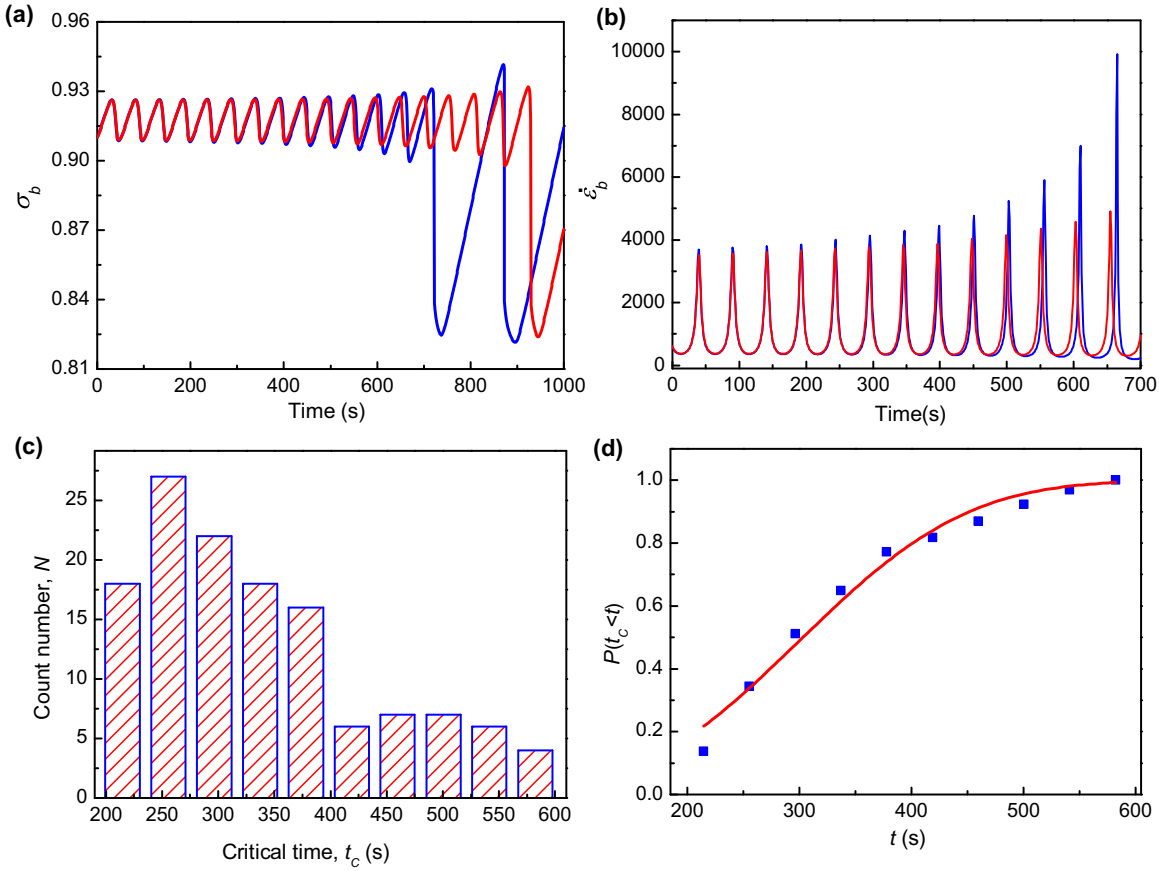

FIG. 5. Numerical calculations illustrating the sensitivity of shear band properties on the initial condition in the chaotic dynamic regime for $k = 100$ and $\dot{\epsilon}_0 = 10^3$. (a) Time evolution of resistant stress σ_b of a shear band under the initial condition (0.91, 0.1975, 0.013) (in the blue line) and (0.91, 0.2, 0.013)(in the red line), respectively. (b) Time evolution of the strain rate within a shear band $\dot{\epsilon}_b$, corresponding to (a). (c) The count number histograms for critical time t_c, when $\dot{\epsilon}_b$ reaches 4500 for the first time for 133 parameter sets of initial conditions from (0.90901, 0.1975, 0.013) to (0.91,0.1975,0.013) with an interval of 0.00001 and from (0.91,0.197,0.013) to (0.91,0.2,0.013) with an interval of 0.001. (d) The cumulative probability distribution of t_c for 133 parameter sets of initial conditions, which can be well fitted by the Weibull distribution with the fitted parameter $\beta = 342.48$ and $m = 3.01$.

other two variables (σ_b and χ) during deformation, making the shear band dynamics become complex. The current finding suggests that the conventional view on the role of temperature rise during the plastic flow of MGs should be reassessed.

In summary, we showed that a single shear band in MGs exhibits complex chaotic dynamics through the combination of experimental and theoretical analysis. We also demonstrated that the experimentally observed large plasticity fluctuation of MGs tested at the same conditions can be interpreted from the chaotic shear-band dynamics, which could lead to an uncertainty on the appearance of the critical condition for runaway shear banding during deformation. Physically, the chaotic shear-band dynamics arises from the interplay between structural disordering and temperature rise within the shear band. By tuning the deformation parameters, the chaotic dynamics can be transformed to a periodic orbit state. This applies to most bulk MGs since their deformation behavior can be dominated by a single primary shear band. For a few MGs whose behavior is dominated by a large number of multiple shear bands, the avalanchelike SOC dynamics resumes. Our results suggest that the plastic flow of MGs is a complex dynamic process, which is highly sensitive to initial conditions and reminiscent of the "butterfly effect" as observed in many complex dynamic systems. Finally, it is worth noting that shear banding process in MGs resembles many dynamic phenomena across different time and length scales, e.g., peeling of adhesive tapes [46], friction and lubrication in industrial process [58], seismic and geodetic fault slip [59], etc. Our current finding may be useful to understanding the complex nature of these dynamic systems, all of which one may encounter in the broad discipline of nature and engineering.

ACKNOWLEDGMENTS

B.A.S. and W.H.W. acknowledge the support from the National Science Foundation of China (NSFC) (Grants No. 51822107, No. 51671121, No. 61888102, No. 51761135125, and No. 51520105001), National Key Research and Development Plan (Grant No. 2018YFA0703603) and the Natural Science Foundation of Guangdong Province (Grant No. 2019B030302010) and Strategic Priority Research Program of Chinese Academy of Sciences (XDB30000000). L.P.Y. thanks the China Postdoctoral Science Foundation (Grant No. 2019M651600) and the High-Level Personal Foundation of

Henan University of Technology (2018BS027). J.L.R. thanks the support from the NSFC (Grant No. 11771407) and the Chinese Academy of Engineering Advisory Project (Grant No. 2020-ZD-16).

[1] C. A. Schuh, T. C. Hufnagel, and U. Ramamurty, Acta Mater. **55**, 4067 (2007).
[2] M. Chen, Annu. Rev. Mater. Res. **38**, 445 (2008).
[3] F. Spaepen, Acta Metall. **25**, 407 (1977).
[4] A. Argon, Acta Metall. **27**, 47 (1979).
[5] M. L. Falk and J. S. Langer, Phys. Rev. E **57**, 7192 (1998).
[6] B. Tyukodi, S. Patinet, S. Roux, and D. Vandembroucq, Phys. Rev. E **93**, 063005 (2016).
[7] C. Maloney and A. Lemaître, Phys. Rev. Lett. **93**, 016001 (2004).
[8] A. Greer, Y. Cheng, and E. Ma, Mater. Sci. Eng: R **74**, 71 (2013).
[9] J.-O. Krisponeit, S. Pitikaris, K. E. Avila, S. Küchemann, A. Krüger, and K. Samwer, Nat Commun **5**, 3616 (2014).
[10] Y. Q. Cheng and E. Ma, Phys. Rev. B **80**, 064104 (2009).
[11] D. C. Hofmann, J.-Y. Suh, A. Wiest, G. Duan, M.-L. Lind, M. D. Demetriou, and W. L. Johnson, Nature (London) **451**, 1085 (2008).
[12] B. Sarac and J. Schroers, Nat. Commun **4**, 2158 (2013).
[13] J. Das, M. B. Tang, K. B. Kim, R. Theissmann, F. Baier, W. H. Wang, and J. Eckert, Phys. Rev. Lett. **94**, 205501 (2005).
[14] P. A. Thompson and M. O. Robbins, Science **250**, 792 (1990).
[15] B. Bhushan, J. N. Israelachvili, and U. Landman, Nature (London) **374**, 607 (1995).
[16] J. S. Langer, J. M. Carlson, C. R. Myers, and B. E. Shaw, Proc. Natl. Acad. Sci. **93**, 3825 (1996).
[17] S. Song, H. Bei, J. Wadsworth, and T. Nieh, Intermetallics **16**, 813 (2008).
[18] J. Antonaglia, W. J. Wright, X. Gu, R. R. Byer, T. C. Hufnagel, M. LeBlanc, J. T. Uhl, and K. A. Dahmen, Phys. Rev. Lett. **112**, 155501 (2014).
[19] D. Klaumünzer, A. Lazarev, R. Maaß, F. H. Dalla Torre, A. Vinogradov, and J. F. Löffler, Phys. Rev. Lett. **107**, 185502 (2011).
[20] Y. Wu, H. Li, Z. Liu, G. Chen, and Z. Lu, Intermetallics **18**, 157 (2010).
[21] B. A. Sun, Y. Yang, W. H. Wang, and C. T. Liu, Sci. Rep. **6**, 21388 (2016).
[22] J. J. Lewandowski, W. H. Wang, and A. L. Greer, Philo. Mag. Lett. **85**, 77 (2005).
[23] D. Jang and J. R. Greer, Nat. Mater. **9**, 215 (2010).
[24] H. Ke, B. Sun, C. Liu, and Y. Yang, Acta Mater. **63**, 180 (2014).
[25] Z. Han, W. Wu, Y. Li, Y. Wei, and H. Gao, Acta Mater. **57**, 1367 (2009).
[26] B. A. Sun, S. Pauly, J. Hu, W. H. Wang, U. Kühn, and J. Eckert, Phys. Rev. Lett. **110**, 225501 (2013).
[27] C. Liu, V. Roddatis, P. Kenesei, and R. Maaß, Acta Mater. **140**, 206 (2017).
[28] B. A. Sun, H. B. Yu, W. Jiao, H. Y. Bai, D. Q. Zhao, and W. H. Wang, Phys. Rev. Lett. **105**, 035501 (2010).
[29] J. L. Ren, C. Chen, Z. Y. Liu, R. Li, and G. Wang, Phys. Rev. B **86**, 134303 (2012).
[30] H. B. Yu, W. H. Wang, J. L. Zhang, C. H. Shek, and H. Y. Bai, Adv. Eng. Mater. **11**, 370 (2009).
[31] P. G. Debenedetti and F. H. Stillinger, Nature (London) **410**, 259 (2001).
[32] E. N. Lorenz, J. Atmos. Sci. **20**, 130 (1963).
[33] G. B. Pasternack, Adv. Water Resour. **23**, 253 (1999).
[34] E. Liz and A. Ruiz-Herrera, SIAM J. App. Dyna. Sys. **11**, 1200 (2012).
[35] A. Akhavan, A. Samsudin, and A. Akhshani, J. Franklin I. **348**, 1797 (2011).
[36] C. Werndl, Brit. J. Philos. Sci. **60**, 195 (2009).
[37] See Supplemental Material at http://link.aps.org/supplemental/10.1103/PhysRevB.101.224111 for chaotic dynamics in shear-band-mediated plasticity of metallic glasses.
[38] A. M. Fraser and H. L. Swinney, Phys. Rev. A **33**, 1134 (1986).
[39] L. Cao, Phys. D (Amsterdam, Neth.) **110**, 43 (1997).
[40] A. Wolf, J. B. Swift, H. L. Swinney, and J. A. Vastano, Phys. D (Amsterdam, Neth.) **16**, 285 (1985).
[41] P. Frederickson, J. L. Kaplan, E. D. Yorke, and J. A. Yorke, J. Differ. Equ. **49**, 185 (1983).
[42] T. H. Courtney, *Mechanical Behavior of Materials* (McGraw-Hill Company, Inc., New York, 2000).
[43] W. F. Wu, Y. Li, and C. A. Schuh, Philos. Mag. **88**, 71 (2008).
[44] B. Sun and W. Wang, Prog. Mater. Sci. **74**, 211 (2015).
[45] R. Maaß, D. Klaumünzer, and J. Löffler, Acta Mater. **59**, 3205 (2011).
[46] R. Sarmah, G. Ananthakrishna, B. Sun, and W. Wang, Acta Mater. **59**, 4482 (2011).
[47] P. Grassberger and I. Procaccia, Phys. D (Amsterdam, Neth.) **9**, 189 (1983).
[48] G. Benettin, L. Galgani, A. Giorgilli, and J.-M. Strelcyn, Meccanica **15**, 21 (1980).
[49] E. G. Daub, D. Klaumünzer, and J. F. Löffler, Phys. Rev. E **90**, 062405 (2014).
[50] W. L. Johnson and K. Samwer, Phys. Rev. Lett. **95**, 195501 (2005).
[51] R. Sarmah and G. Ananthakrishna, Acta Mater. **91**, 192 (2015).
[52] A. Lemaître and J. Carlson, Phys. Rev. E **69**, 061611 (2004).
[53] C. Liu, A. Das, W. Wang, S. Küchemann, P. Kenesei, and R. Maaß, Scrip. Mater. **170**, 29 (2019).
[54] R. Conner, Y. Li, W. Nix, and W. Johnson, Acta Mater. **52**, 2429 (2004).
[55] R. D. Conner, W. L. Johnson, N. E. Paton, and W. D. Nix, J. Appl. Phys. **94**, 904 (2003).
[56] J. S. Langer, Phys. Rev. E **70**, 041502 (2004).
[57] W. J. Wright, M. Samale, T. Hufnagel, M. LeBlanc, and J. Florando, Acta Mater. **57**, 4639 (2009).
[58] M. Urbakh, J. Klafter, D. Gourdon, and J. Israelachvili, Nature (London) **430**, 525 (2004).
[59] J. M. Carlson and J. S. Langer, Phys. Rev. Lett. **62**, 2632 (1989).